Measuring Horizontal Ground Deformation Using Optical Satellite Images Part 1 of 2

Sébastien Leprince

California Institute of Technology

Ge 167 Lecture Notes
May 12, 2009

Overview

- Objective: Monitoring natural phenomena involving Earth's surface dynamics, e.g., earthquakes, volcanoes, glacier flow, landslides, sand dunes migration, etc...
- Motivation: To validate/calibrate/refine physical models. To improve early evaluation of damage for large disasters
- Approach: Measuring horizontal ground deformations from optical satellite images: SPOT 1-2-3-4 (10 m), SPOT 5 (5 m and 2.5 m), ASTER (15 m), Quickbird (0.7 m), Aerial photographs (0.25-1 m)

Measuring deformation: a toy example

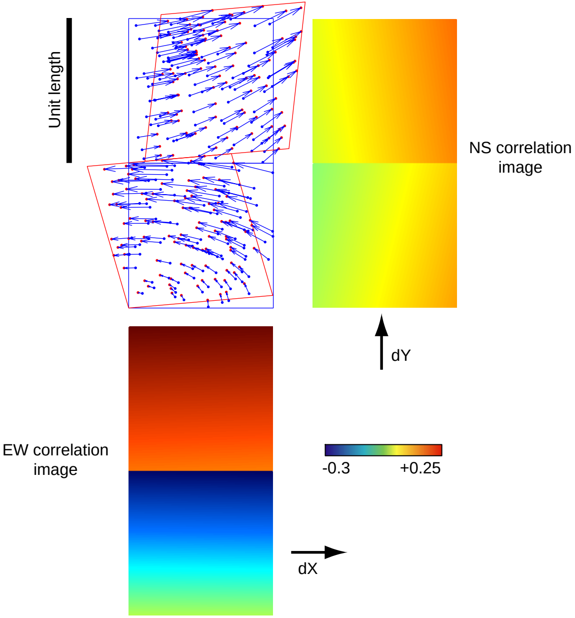

Measuring Horizontal Ground Displacement, Methodology Flow

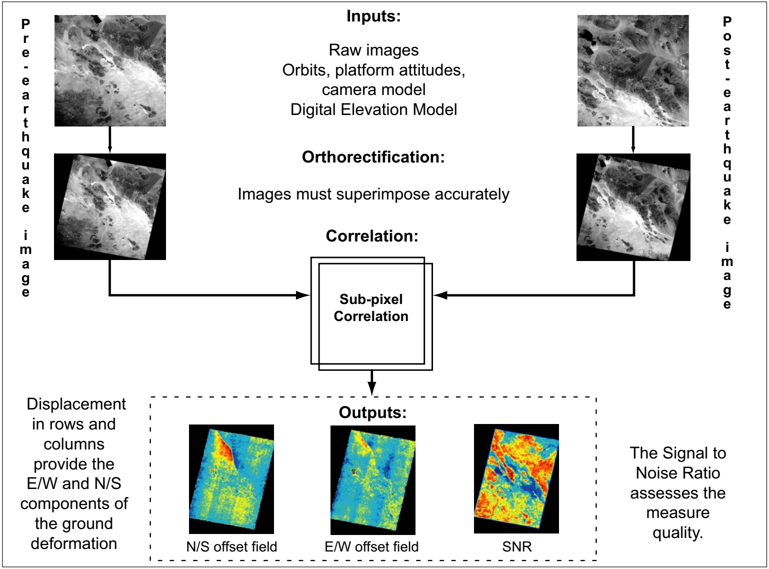

The 1999 Mw 7.1 Hector Mine Earthquake

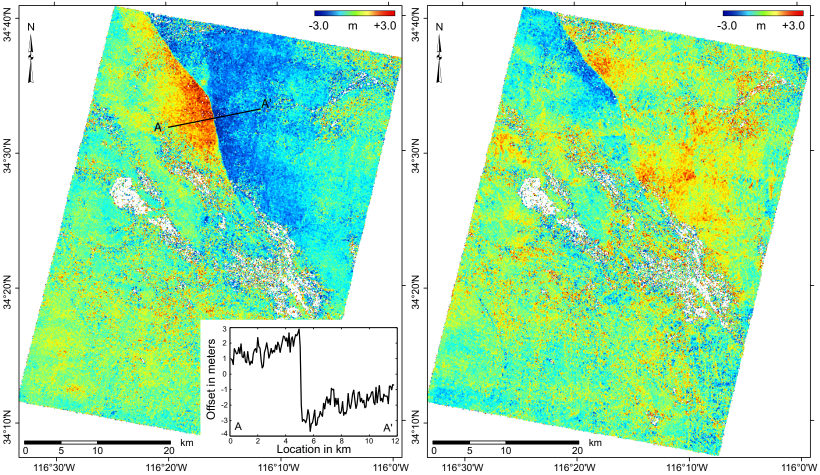

The Hector Mine horizontal coseismic field (NS and EW) derived from 10m SPOT4 1998 and 10m SPOT2 2000 images.

In this 2-session lecture + 1 lab, you will (should...) learn:

- The basic theories, methodologies, and trade-offs involved to produce horizontal deformation maps from optical data,
- How to interpret/estimate the quality of the deformation maps produced by understanding potential biases,
- How to use the COSI-Corr (Co-registration of Optically Sensed Images and Correlation) software, which will assist you in all the processing tasks involved.

The viewing geometry of optical sensors

Questions: Identify the move between these two shots. What did your brain had to do to come up with the solution?

The viewing geometry of optical sensors

Image acquired with almost similar viewing geometries

The viewing geometry of optical sensors

Image acquired with almost similar viewing geometries

Images must be compared in the same geometry

- Images must be re-projected in a common geometry to be compared. Infinitely many possible projections: any arbitrary common viewing geometry is theoretically valid: in which geometry images should be analyzed?
- Try to find a viewing geometry that minimizes geometrical "stretch" on both images during re-projection: application dependent, but global trends exist:
  - Radar interferometry: images acquired with short baseline. Almost similar viewing geometry, common viewing geometry defined as the viewing geometry of one of the images (master/slave)
  - Same idea also encountered for optical sensors. However, optical sensors have no baseline constraints and images can have very different viewing geometries. Can define an "intermediate" viewing geometry, independent of the images (more flexible to compare images from several different sensors). Images analyzed in orthorectified geometry.

SAR vs Optical viewing geometries

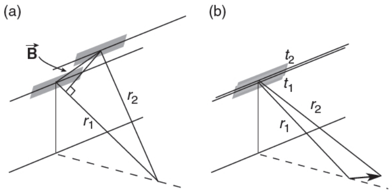

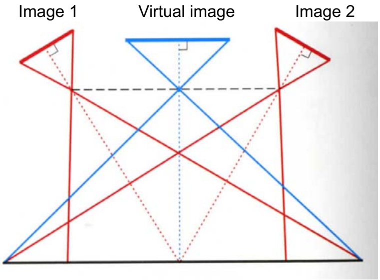

SAR images are usually analyzed (e.g., InSAR applications) by taking one of the image as the reference geometry. Due to the largest disparities in viewing geometries, optical images are usually analyzed using intermediate projections. They are commonly orthorectified, meaning that they are reprojected on the ground, accounting for the topography. In Orthoimages, each pixel is as if it was seen exactly from above. Proper projection of images depends on the proper modeling of the acquisition sensor.

Common types of optical sensor geometries

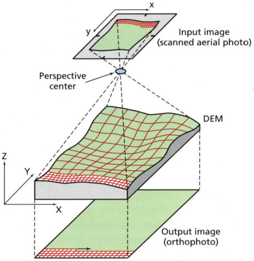

Acquisition geometry of a frame camera. The image is acquired in a single shot. Archive images are film-based and need to be scanned to be processed; more modern cameras use digital frame sensors.

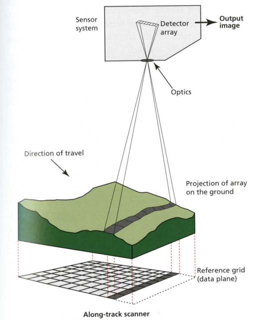

Figure 6.11 Along-track or pushbroom scanner. The pixels of an entire swath width are captured at one time, so the image is built up a row at a time in the direction of travel, i.e., along the ground track.

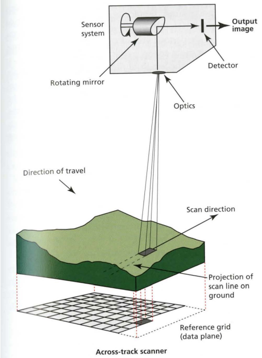

Figure 6.3 Across-track or whiskbroom scanner. An across-track scanner builds up an image one pixel at a time as it scans the terrain perpendicular to the direction of travel.

- Frame camera: very high resolution imaging (1-100 cm GSD), limited footprint (1-10 km) - aerial surveys, old spy satellites, etc...
- Pushbroom systems (main focus in this lecture): high resolution imaging (0.5-3 0m GSD), medium swath width (15-60km) - SPOT, ASTER, Quickibird, Ikonos, etc...
- Whiskbroom systems: medium-low resolution (30-1000 m GSD), large swath (100-1000 km), multispectral - Landsat, Modis, AVHRR, etc...

Orthorectification Model

Pushbroom acquisition geometry

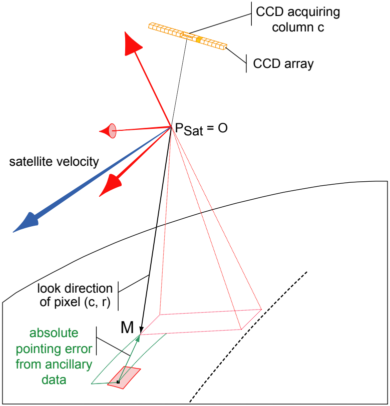

- O, optical center in space
- M, ground point seen by pixel p
- $\vec{u}_1$ pixel pointing model
- $R(p)$ 3D rotation matrix, roll, pitch, yaw at p
- $T(p)$ Terrestrial coordinates conversion
- $\vec{\delta}$ correction on the look directions to insure coregistration
- $\lambda > 0$

$$M(p) = O(p) + \lambda \left[\underbrace{T(p)R(p)\vec{u}_1(p)}_{\vec{u}_3(p)} + \vec{\delta}(p) \right]$$

Orthorectification: Look Direction Correction

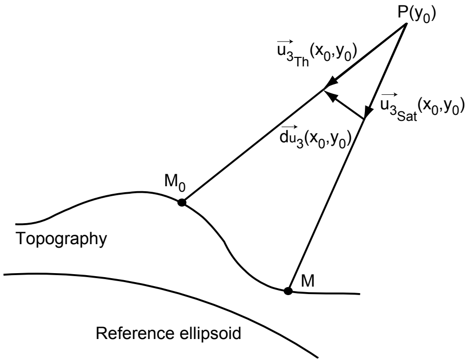

Look direction discrepancy

$$\vec{\delta}(p) = \overrightarrow{du}_3(x_0, y_0) = \vec{u}_{3_{Th}}(x_0, y_0) - \vec{u}_{3_{Sat}}(x_0, y_0)$$

Ground Control Point GCP:
$\{p(x_0, y_0), M_0\}$

Orthorectification: An Irregular Mapping

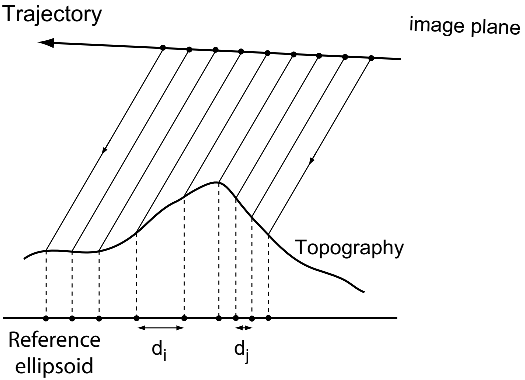

Image pixels are assumed to regularly sample the image plane, but they sample the ground irregularly

Orthorectification: An Irregular Mapping

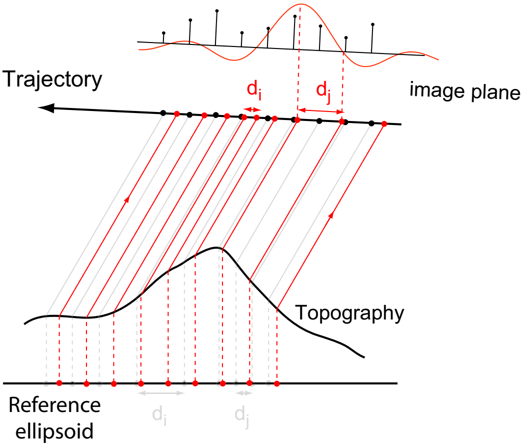

We introduce an inverse mapping to facilitate resampling

Orthorectification: An Irregular Mapping

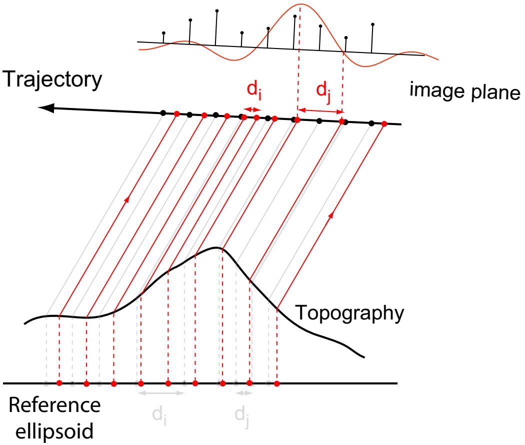

To avoid aliasing in the resampled signal, ideal resampling kernel:

$$h_d(x) = \frac{\sin \frac{\pi x}{d}}{\frac{\pi x}{d}}, \qquad \text{with } d = \max(1, \{d_i\})$$

Orthorectification: Inverse Model Principle

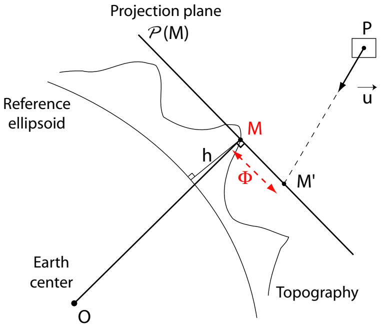

Solution: find pixel (x, y) that minimizes

$$\Phi(x, y) = \|\overrightarrow{OM} - \overrightarrow{OM'}(x, y)\|^2$$

with

$$\overrightarrow{OM'}(x, y) = \overrightarrow{OP}(y) + \lambda^* \cdot \vec{u}(x, y)$$

and λ^* such that M' belongs to $\mathcal{P}(M)$

Given M, which pixel (x, y) saw M?

Resampling: general approach

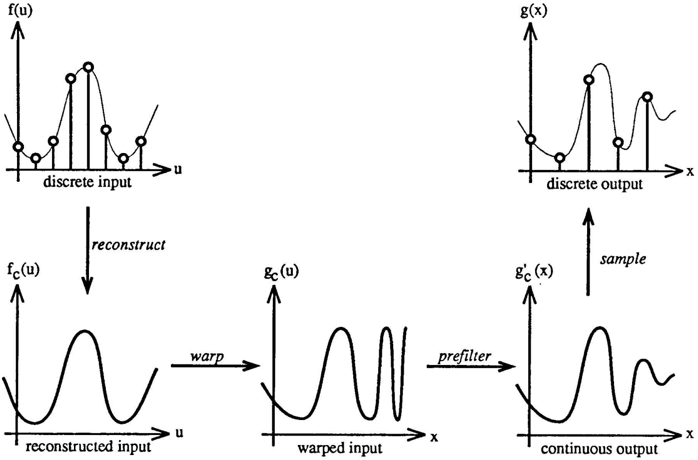

Figure 3.11: *The four steps of ideal resampling: reconstruction, warp, prefilter, and sample.*

Resampling: practical implementation

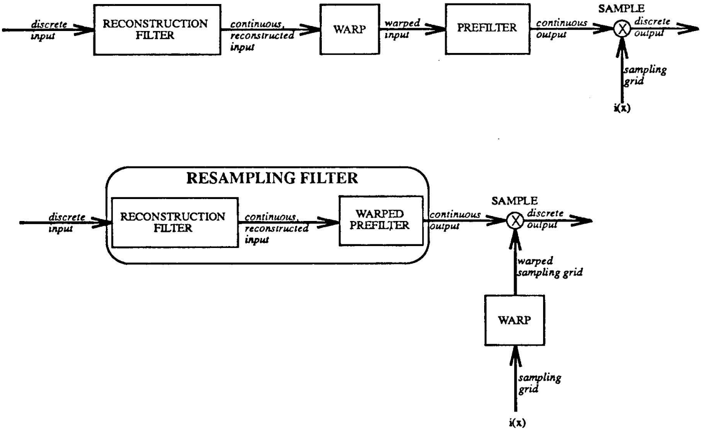

Figure 3.12: *Resampling filter block diagram. Top: conceptual model. Bottom: implementation.*

Resampling: 1D ideal case

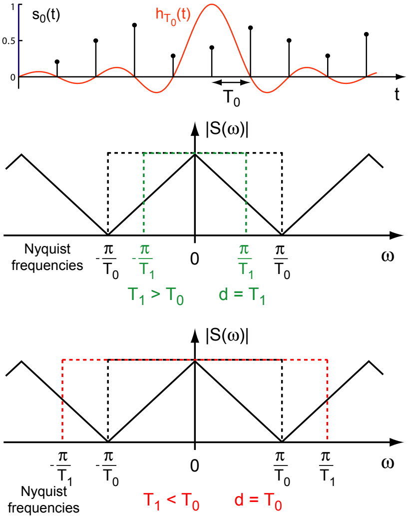

$s_0(t)$ bandlimited at Nyquist frequency $\frac{\pi}{T_0}$, to be resampled at a new sampling period T_1

Ideal resampling kernel:

$$h_d(t) = \frac{\sin \frac{\pi t}{d}}{\frac{\pi t}{d}}$$

To avoid aliasing in the resampled signal:

- $d = \max(T_0, T_1)$

d effective signal "resolution"

Resampling: popular convolution-based interpolation kernels

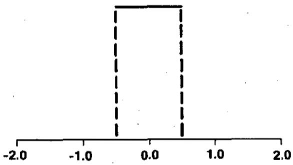

Nearest-Neighbor

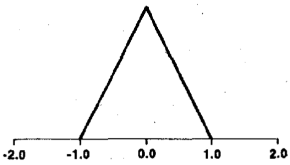

Linear

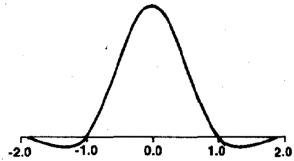

Piecewise-cubic

Ortho-Resampling: a simple particular case using NN kernel

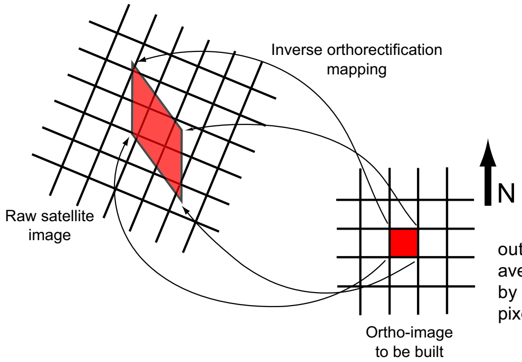

output pixel = area weigthed average of input pixels covered by inverse mapping of output pixel

- Kernel locally warped according to local mapping warp (warping usually linearized locally = Jacobian of ortho-mapping)

- In practice, use higher order (sinc-like) kernels for better resampling quality

Image Correlation: problem formulation

Given two images i_1 and i_2 such that

$$i_2(x, y) = i_1(x - \Delta_x, y - \Delta_y)$$

how to retrieve the translation (Δ_x, Δ_y)?

Generally, problem formulated as:

Find (Δ_x, Δ_y) such that $S(i_1(x, y), i_2(x + \Delta_x, y + \Delta_y))$ is maximum, for some similarity measure S.

- Which similarity measure S should we use?
- How to achieve sub-pixel accuracy?

Image Correlation: popular similarity measures

- Sum of Squared Differences (SSD)

$$SSD_{i_1,i_2}(\Delta_x, \Delta_y) = \sum_{N_x} \sum_{N_y} [i_1(x,y) - i_2(x+\Delta_x, y+\Delta_y)]^2$$

for N_x and N_y centered about x and y

- Normalized Cross-Correlation (NCC), or Correlation Coefficient

$$NCC_{i_1,i_2}(\Delta_x, \Delta_y) = \frac{\sum_{N_x} \sum_{N_y} (i_1(x,y) - \bar{i}_1)(i_2(x+\Delta_x, y+\Delta_y) - \bar{i}_2)}{\sqrt{\sum_{N_x} \sum_{N_y} (i_1(x,y) - \bar{i}_1)^2 \sum_{N_x} \sum_{N_y} (i_2(x+\Delta_x, y+\Delta_y) - \bar{i}_2)^2}}$$

- Phase Correlation based on Fourier Shift Theorem

$$i_2(x,y) = i_1(x-\Delta_x, y-\Delta_y) \Rightarrow I_2(\omega_x, \omega_y) = I_1(\omega_x, \omega_y) e^{-j(\omega_x \Delta_x + \omega_y \Delta_y)}$$

$$\mathcal{F}^{-1}\left\{ \frac{I_1(\omega_x, \omega_y) I_2^*(\omega_x, \omega_y)}{|I_1(\omega_x, \omega_y) I_2^*(\omega_x, \omega_y)|} \right\} = \mathcal{F}^{-1}\left\{ e^{j(\omega_x \Delta_x + \omega_y \Delta_y)} \right\} = \delta(x+\Delta_x, y+\Delta_y)$$

Image Correlation: popular similarity measures

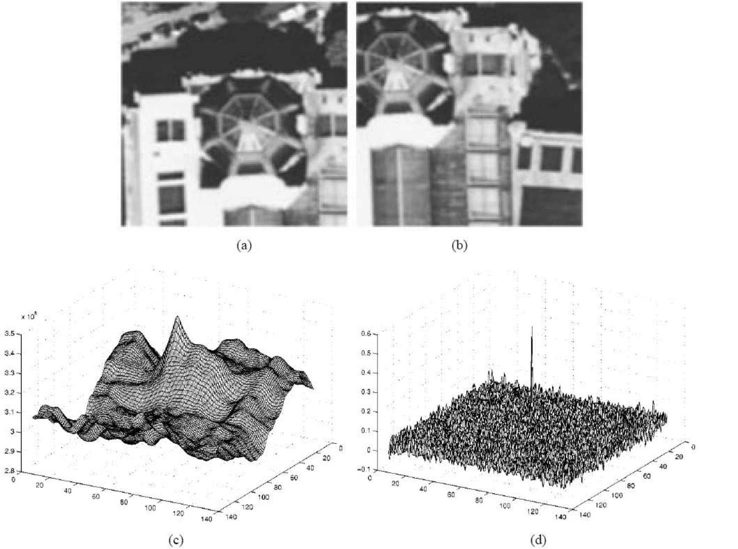

Fig. 1. (a) and (b) Aerial images of Paris with displacements along both axes, (c) standard cross-correlation, and (d) phase correlation.

Image Correlation: subpixel accuracy

- Correlation surface computed for integer values of (Δ_x, Δ_y) comprised in a search area. Then interpolation of the correlation surface near the maximum, or fit to a smooth surface, e.g., Gaussian. Easy implementation but not very accurate because interpolation model for correlation surface not always well known.

- By introducing a subpixel shift between images to be correlated via interpolation/resampling. The image is shifted by resampling, the goal being to find the best resampling shift that maximizes the similarity function. Implementation more complex but accuracy can be up to an order of magnitude better than previous method.

- If we solve the registration problem in the Fourier domain directly, image resampling becomes implicit and can lead to faster algorithms using FFT (best of both worlds?).

Image Correlation: what we do in COSI-Corr

- Fourier Shift Theorem

$$i_2(x,y) = i_1(x-\Delta_x, y-\Delta_y)$$
$$I_2(\omega_x,\omega_y) = I_1(\omega_x,\omega_y)e^{-j(\omega_x\Delta_x+\omega_y\Delta_y)}$$

- Normalized Cross-spectrum

$$C_{i_1i_2}(\omega_x,\omega_y) = \frac{I_1(\omega_x,\omega_y)I_2^*(\omega_x,\omega_y)}{|I_1(\omega_x,\omega_y)I_2^*(\omega_x,\omega_y)|} = e^{j(\omega_x\Delta_x+\omega_y\Delta_y)}$$

- Finding the relative displacement

$$\phi(\Delta_x,\Delta_y) = \sum_{\omega_x=-\pi}^{\pi}\sum_{\omega_y=-\pi}^{\pi} W(\omega_x,\omega_y)|C_{i_1i_2}(\omega_x,\omega_y) - e^{j(\omega_x\Delta_x+\omega_y\Delta_y)}|^2$$

W weighting matrix. (Δ_x,Δ_y) such that ϕ minimum.

Image Correlation: so which similarity measure is best finally?

- The NCC method usually performs better than the SSD because it is insensitive to linear transformations in image intensities. Indeed, photometric differences due to change in illumination, which are always encountered in practice with images acquired at different time, can be locally modeled as linear contrast changes.

- NCC and SSD are based on second order statistics and can be viewed, from a Bayesian approach, as the best solution when images are corrupted with additive Gaussian white noise. In other words, these methods consider that the displacement to be found is exact, and that images amplitude only, contains noise.

- Normalized phase correlation methods are also insensitive to linear contrast change. However, the noise formulation is quite different. From a Bayesian point of view, the noise can be considered Gaussian-like on the displacement, while images are considered noise free! Indeed, we can write:

  $$\Phi(\Delta) = \sum_{\omega} |e^{j\omega\Delta_x} - e^{j\omega\Delta}|^2 = 2\sum_{\omega}[1 - \cos(\omega(\Delta - \Delta_x))]$$

  Then minimizing Φ is equivalent to maximizing, over Δ,

  $$\frac{\prod_{\omega} e^{W'(\omega)\cos(\omega(\Delta - \Delta_x))}}{C(\omega)}.$$

  This is Von-Mises distribution on the phase shift, then Gaussian-like distribution on Δ.

Image Correlation: so which similarity measure is best finally?

- Conclusion: The phase correlation method will provide more accurate results when the images have a low noise level, and when some deviation from the rigid translation model is expected. This is often the case in practice and the measure provided can be seen as the average displacement over the correlation window.

- At high noise level, NCC methods usually perform better than phase correlation methods, but using iterative re-weighted methods on W mitigates the strong noise-free requirement of the images in the phase correlation formulation and adds some robustness to the solution.

Processing Chain

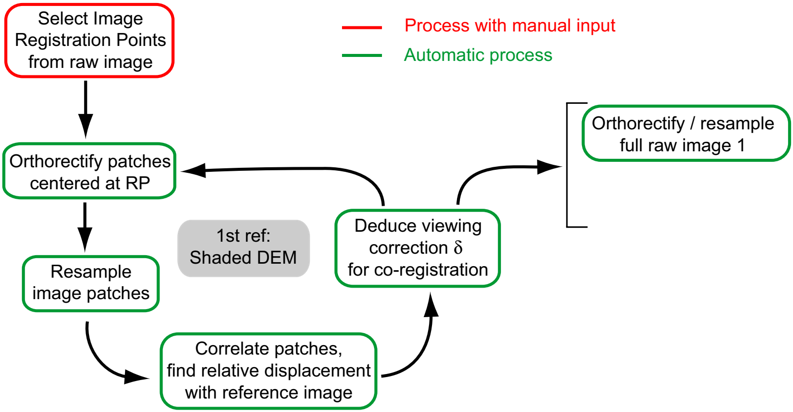

Processing Chain

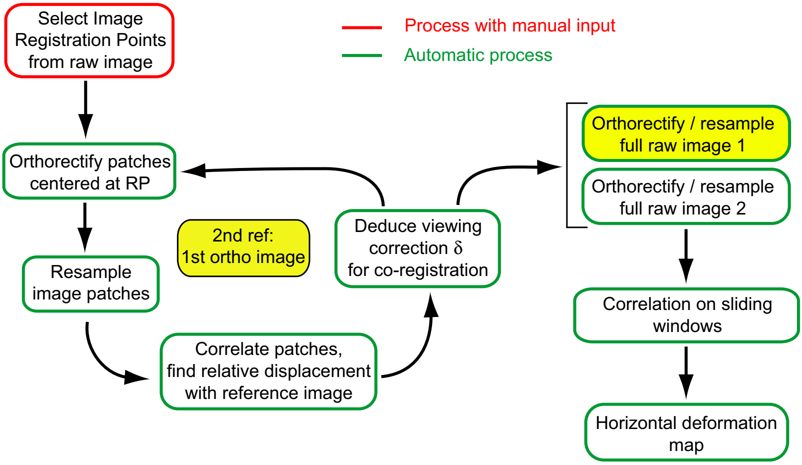

1999 Mw 7.1 Hector Mine Earthquake, CA

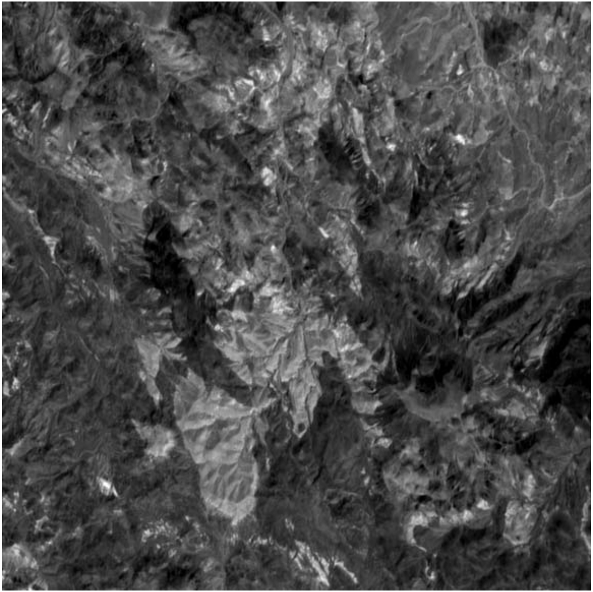

1999 Mw 7.1 Hector Mine Earthquake, CA

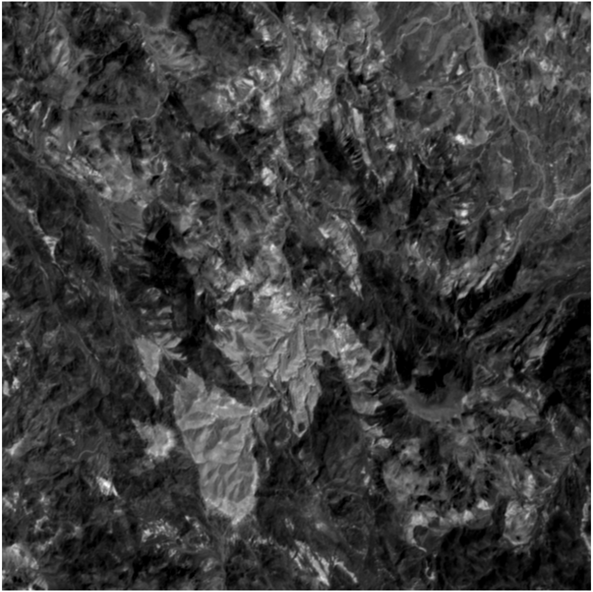

1999 Mw 7.1 Hector Mine Earthquake, CA

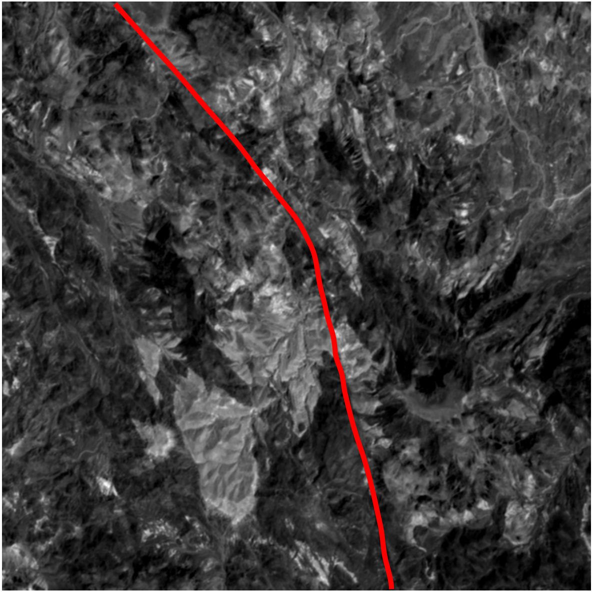

The 1999 Mw 7.1 Hector Mine Earthquake

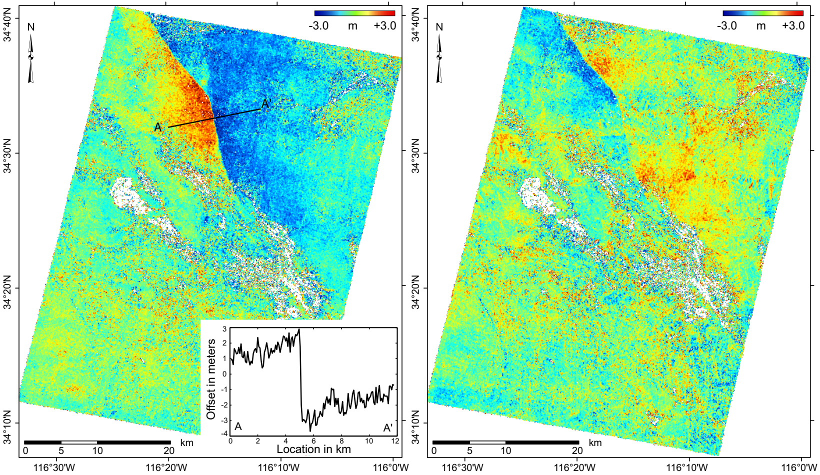

The Hector Mine horizontal coseismic field (NS and EW) derived from 10m SPOT4 1998 and 10m SPOT2 2000 images.

The 1999 Mw 7.1 Hector Mine Earthquake

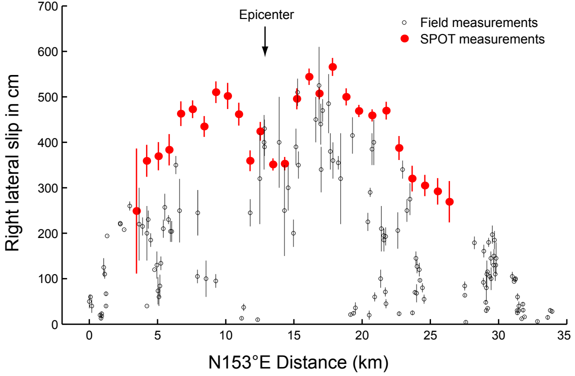

- Horizontal slip vectors measured from linear least square adjustment on each side of the fault. Perpendicular profiles are stacked over a width of 880 m and a length of 8 km.

Field measurements from J.A. Treiman et al., BSSA, 2002

The 1999 Mw 7.1 Hector Mine Earthquake

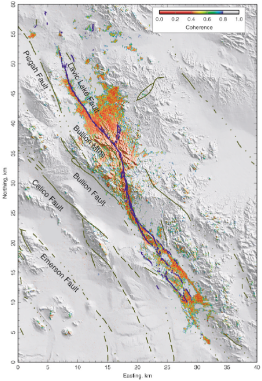

Figure 2. Interferometric coherence, C, for IP1, with $C > 0.8$ set to be transparent. Brown lines indicate known faults (Jennings, 1994). Surface rupture as observed in the field is indicated by the blue line (Treiman *et al.*, 2002). UTM zone 11 projection with origin at (116.457W 34.250N).

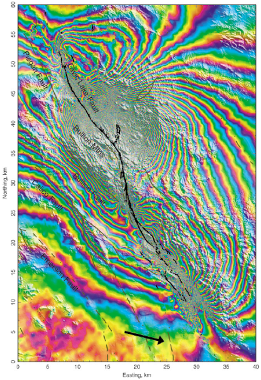

Figure 3. Same as Fig. 2 but color indicates wrapped phase for IP1. Each color cycle represents 2.8 cm of motion in the line-of-sight (LOS) direction. The black arrow represents the horizontal projection of the LOS vector toward the satellite.

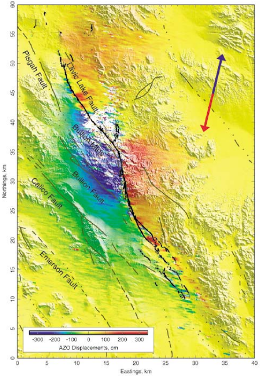

Figure 5. Same as Fig. 3, but color indicates AZO observations. Arrows represents the horizontal component of motion indicated by the respective colors.

M. Simons et al., BSSA, 2002

Optical Correlation and SAR Complementarity

- Optical Image Correlation:
  - The larger the displacement, the higher the technique SNR. Technique mostly usefully to measure large deformation gradients,
  - Mostly sensitive to horizontal component of ground deformation,
  - Can be used to measure change over long time periods,
  - Images from sensors with different geometry, orbit, and resolution can be correlated, potentially huge archive
  - Can correlate on sand, ice even with some ice melt (passive sensor)
  - Images contain aliasing, which limits correlation accuracy
  - Very sensitive to weather condition (clouds), no night imaging for visible bands
- SAR:
  - Amplitude correlation on speckle pattern
  - Azimuth (and range) offsets
  - Fairly insensitive to weather conditions + night and day imaging
  - Analysis only from images acquired with identical geometry. Shadow casting depends on radar orientation and surface reflection properties
  - Images with little aliasing
  - Little backscattering on sand, or different backscattering on ice melt
  - InSAR:
    - Sensitive to ground deformation in range direction
    - Very accurate but loss of coherence when displacement gradient too large (depends on radar wavelength and pixel size),
    - Temporal decorrelation due to change in scatterer geometry
    - Path delays due to tropospheric/ionospheric structure